

Title	Frost damage to roof tiles: Ice distribution in freeze-thaw experiment
Author(s)	Ueda, Ayumi; Iba, Chiemi; Hokoi, Shuichi
Citation	Energy Procedia (2015), 78: 2542-2547
Issue Date	2015-11
URL	http://hdl.handle.net/2433/215119
Right	© 2015 The Authors. Published by Elsevier Ltd. This is an open access article under the CC BY-NC-ND license(http://creativecommons.org/licenses/by-nc-nd/4.0/).
Type	Journal Article
Textversion	publisher

6th International Building Physics Conference, IBPC 2015

Frost damage to roof tiles: Ice distribution in freeze-thaw experiment

Ayumi Ueda^{a,*}, Chiemi Iba^a, Shuichi Hokoi^a

^a*Kyoto University, Graduate School of Engineering, Kyoto daigaku-katsura, Nishikyo-ku, Kyoto 615-8540, Japan*

Abstract

In this paper, frost damage to roof tiles, which is among the most serious causes of deterioration, was discussed. Freeze-thaw experiments were conducted and frost damages similar to that observed in a field survey were reproduced. The experimental results were examined by numerical analysis focusing on ice content distribution and temperature.

© 2015 The Authors. Published by Elsevier Ltd. This is an open access article under the CC BY-NC-ND license (<http://creativecommons.org/licenses/by-nc-nd/4.0/>).

Peer-review under responsibility of the CENTRO CONGRESSI INTERNAZIONALE SRL

Keywords: frost damage; roof tile; water content distribution; ice content distribution; freeze-thaw experiment.

1. Introduction

Freeze-thaw cycles are among the most serious causes of roof tile deterioration. Therefore, many researchers have developed roof tile materials with high frost resistance, which has led to improved tile production processes and better roof preservation. Nonetheless, roof tiles remain susceptible to frost damage, even in relatively warm areas, such as Kyoto, Japan, where the average winter outdoor temperature is approximately 5 °C. To efficiently manage frost damage, we must understand how the materials deteriorate under climatic impacts and identify the factors that influence frost damage. The final aim of our research is to clarify the behavior of roof tiles under climatic impacts and to predict the physical deterioration process by numerical modelling.

We have conducted a field survey on fence roof tiles in an old temple precinct in Kyoto, Japan. Figure 1 shows a schematic of the upper part of a fence structure there. Several types of deterioration were observed in each roof part, including cracks, flaking and delamination [1]. In the following section, eave-end tile used at the survey site was adopted as an experimental specimen. The deteriorations observed in eave-end tiles are shown in Figure 2. Eave end

* Corresponding author. Tel.: +81-75-383-2920; fax: +81-75-383-2920.

E-mail address: be.ayu@archi.kyoto-u.ac.jp

tiles were prone to flaking on convex part (i) and back side (ii). More severe exfoliation (iii) or cracks (iv) were also observed in several tiles.

In this study, we conducted freeze-thaw experiments in which we attempted to reproduce the frost damage observed in the field survey. Based on the experimental results, the ice distribution in the roof tile during the freezing-thawing processes was calculated using numerical analysis.

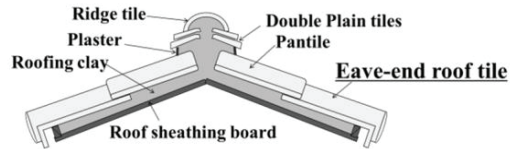


Fig. 1. The upper part of the surveyed fence structure (section).

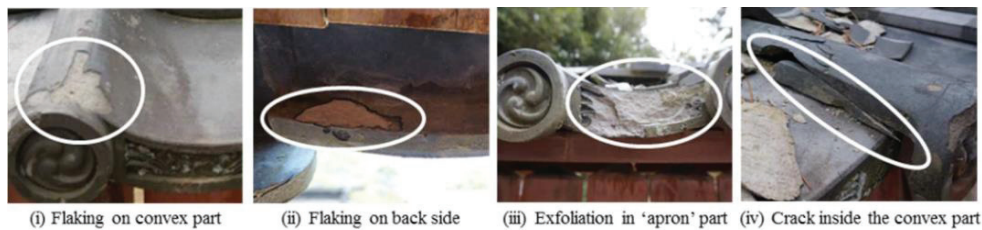


Fig. 2. Distinctive deterioration of eave-end tiles.

Nomenclature		Subscript	
T	absolute temperature [K]	w	water
T_o	freezing temperature of free water [K]	s	solid
c	specific heat [J/(kgK)]	g	gas
t	time [s]	l	liquid
β	thermal conductivity [W/(mK)]	i	ice
ρ	density [kg/m ³]		
μ	moisture content [m ³ /m ³]		
μ	water chemical potential (relative to free water state) [J/kg]		
β'_T	moisture conductivity by temperature difference [kg/(msK)]		
β'_μ	moisture conductivity by water chemical potential difference [kg/ms(J/kg)]		

2. Freeze-thaw experiments

To evaluate the damage to roof tiles, a series of freeze-thaw experiments were designed and conducted.

2.1. Outline of experiment

A diagram of the experimental setup is shown in Figure 3 (a). We used eave-end tile, which was already damaged to some extent, as an experimental specimen. Although an eave-end tile is usually placed on roof clay, the underside of the tile is partly exposed to air (see Fig. 1). To simulate the actual situation, the center part of the tile contacted the clay surface, and the peripheral part was exposed to air. At first, the clay was fully saturated with water, and the moisture content (mass by mass) of the tile body was 15.03% (not saturated). Figure 3 (b) shows the temperature

and water chemical potential of the air in the test chamber and of the clay during the experiment. The temperature and water chemical potential of the clay was measured using dielectric water potential sensors (MPS-2, Decagon Devices). One cycle was 12 hours, and the experiment was conducted for 10 cycles.

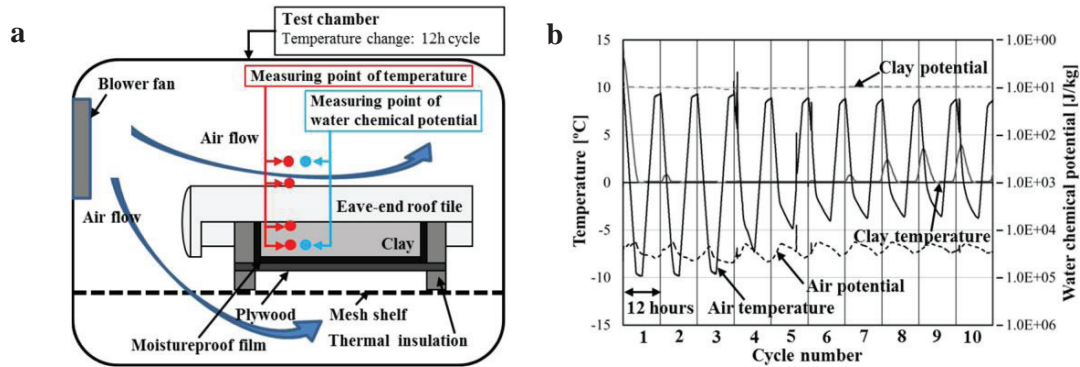


Fig. 3. Experimental conditions: (a) Diagram of experimental setup; (b) Boundary conditions (air in test chamber and clay).

2.2. Results of experiment

In the experiment, serious deterioration occurred, and the processes are presented in Figure 4. Similar to the field situation, flaking could be observed on the back side (i) and (ii), 'apron' part (iii), and convex part (iv). Except for one case of flaking on the back side (i), all flakings were located in the peripheral part, which did not contact the clay. Unlike the field survey, cracks were not observed.



Fig.4. Damage to specimens, observed in the experiment.

Figure 5 shows the temperature of the upper and lower surfaces of the test tile. Several rapid temperature increases seen in Figure 5 were caused by taking the tile out of the test chamber for observation and taking photographs. The upper surface temperature dropped to 3–4°C below zero in the earlier 3 cycles and afterwards temperature dropped slightly below 0 °C. In contrast, the lower surface did not drop below zero.

These results show that the tile temperature in the area apart from the clay is affected by the ambient cold air, and freezing can occur even though the area is not fully saturated. In contrast, the tile temperature in the area close to the clay hardly dropped below zero because of heat generation accompanied by freezing in the clay. Thus, freezing occurred only when the area was fully saturated.

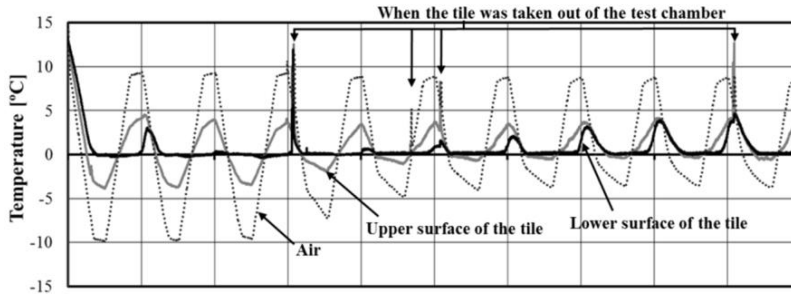


Fig. 5. Temperature profile of the upper and lower surfaces of the tile.

3. Numerical analysis of the freezing-thawing process

We conducted a numerical analysis to examine the ice content distribution in the roof tile during the freezing - thawing processes.

3.1. Basic equations

The equations for simultaneous heat and moisture transfer, which consider freezing and thawing, are used in the analysis [2]. The basic equations are as follows. Equations (1), (2) and (3) are the moisture balance, energy balance and freezing condition, respectively.

$$\left(\frac{\partial \rho_l \Psi_l}{\partial t} \right) \frac{\partial \mu}{\partial x} = \frac{\partial}{\partial x} \left(\lambda' \frac{\partial \mu}{\partial x} \right) + \frac{\partial}{\partial x} \left(\lambda' \frac{\partial \mu}{\partial x} \right) + \lambda' \frac{\partial \mu}{\partial x} - \frac{\partial \rho \Psi}{\partial t} \quad (1)$$

$$c \rho \Psi \frac{\partial T}{\partial t} = \frac{\partial}{\partial x} \left(\lambda \frac{\partial T}{\partial x} \right) + \frac{\partial}{\partial x} \left(\lambda' \frac{\partial T}{\partial x} \right) + \lambda' \frac{\partial T}{\partial x} - H \frac{\partial \rho \Psi}{\partial t} \quad (2)$$

where $c \rho \Psi = c_g \rho_g \Psi_g + c_l \rho_l \Psi_l + c_i \rho_i \Psi_i$,

$$\mu = H_{li} \log_e \left(\frac{T}{T_0} \right) \quad (3)$$

3.2. Calculation model and material properties

Figure 6 shows the calculation model of the experiment. Model 1 is used for the center part of the tile, which contacts the clay. Model 2 shows the peripheral part, where both sides are exposed to air. Both models assume one-dimensional analyses. The air temperature and humidity measured in the experiment are set as boundary conditions (see Fig. 3 (b)). The combined heat transfer coefficients (α) of both sides are determined considering the air velocity in the chamber. The heat and moisture transfer properties of the tile body [3] and the clay [2] are shown in Table 1. The initial temperature is set at 2°C. The initial water chemical potential of the tile body and clay are set at -810 [J/kg] and -10 [J/kg], respectively. These are determined based on the experimental results. The initial degree of saturation of the tile body is about 60%.

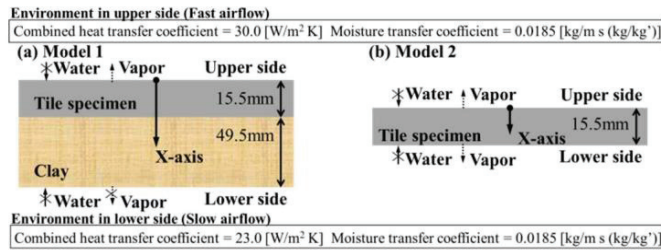


Fig. 6. Calculation model: (a) the center part; (b) the peripheral part

Table 1. Heat and moisture transfer properties of tile body and clay.

Properties	Units	Tile	Clay
Thermal conductivity (dry condition)	W/m K	0.937	0.384
Vapor permeability (50%RH average)	kg/m s Pa	3.84×10^{-12}	3.51×10^{-10}
Water permeability (saturated condition)	kg/m s Pa	3.73×10^{-9}	2.02×10^{-6}
Specific heat	J/kg K	920	1030
Density	kg/m ³	1970	1250
Porosity (= maximum moisture content)	%	26.2	37.2

3.3. Calculated results

The time profiles of temperature, ice content in the tile and the change in ice content distribution in the tile are shown in Figures 7 and 8. These figures show the results of Models 1 and 2, respectively.

In Figure 7 (a), the upper side temperature decreases below zero, whereas the temperature of the lower side is maintained at about 0°C. The surface layer exposed to air is affected by the periodical temperature change of the ambient air. In contrast, in the surface layer in contact with clay, the temperature hardly drops below zero because of the heat capacity of clay and water contained in clay. Although the range of fluctuation is small, it changes similarly to the measured temperature (see Figure 5). Figures 7 (b) and (c) show that freezing occurs periodically in the upper surface layer first and that ice crystals subsequently proceed to the lower surface. In surface layer in contact with clay, although moisture from wet clay infiltrates the bottom surface and causes local high moisture content, ice is not significantly formed.

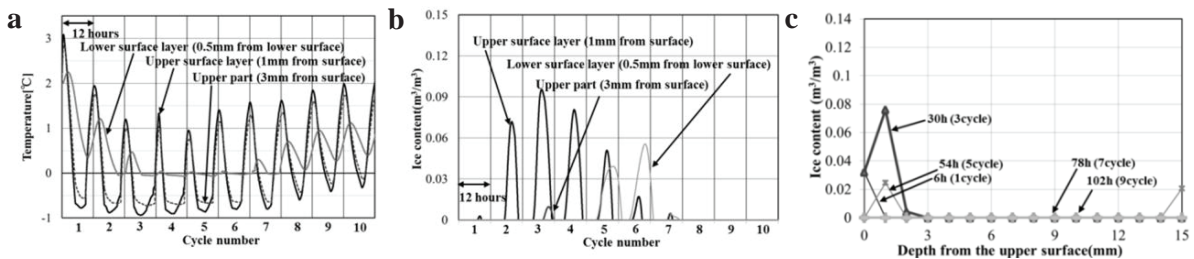


Fig. 7. The results in the case of Model 1 : (a) temperature profile; (b) ice content profile; (c) ice content distribution.

Figure 8 (a) shows that the temperature of the inside part is kept at about -0.7°C for first few cycles and then fluctuates between -1°C and 0.5°C, and that the temperature of both surface layers change periodically. In Figure 8 (b), first, freezing occurs periodically in both surface layers. The amount of ice crystals in the upper layer increases for two cycles and then decreases, whereas that in the lower layer decreases from the beginning. Unlike Figure 7 (b), significant ice crystals continue growing deep into the tile body for several cycles and gradually decrease. Once the

ice formation occurs there, the temperature is maintained at freezing point for several cycles, and water chemical potential in this area is kept low during ice crystal growing. When the ice in a neighboring zone melts, liquid water flows into the freezing zone and the ice crystal remains growing for a while. The areas with maximum ice content move from both surface layers (3 cycles) to the middle part (7 cycles). Furthermore, the amount of ice crystal in Model 2 is more than that in Model 1. It is because that temperature of the tile was kept lower in Model 2 and the duration of ice formation was longer.

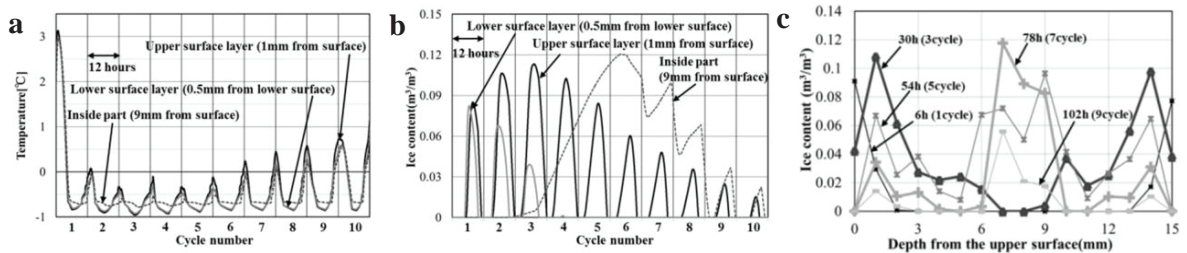


Fig. 8. The results in the case of Model 2 : (a) temperature profile; (b) ice content profile; (c) ice content distribution

4. Discussion

The position of deterioration is examined by comparing calculated ice content distribution to the experimental results. A lot of flakings in the surface area observed in the experiment seem to correspond to the periodical ice formation in the calculation. In the area in contact with wet clay, calculated results show a little amount of ice could be formed and very thin flaking was observed in the experiment. In the area inside the tile body, deterioration could not be recognized in the experiment. However, the numerical analysis shows that freezing could occur there. Severe cracks and delamination observed in the field survey might be caused by such an inside ice formation.

5. Conclusion

In this paper, we conducted a freeze-thaw experiment and a numerical analysis focusing on ice content distribution. We experimentally reproduced frost damage similar to that observed in a field survey and examined the experimental results by numerical analysis. Depending on the position of the tile, the temperature, moisture flow and water content are different, and consequently the ice contents are quite different. In the surface area, the positions of deterioration observed in the experiment correspond to the calculated ice content distribution.

In future studies, we will investigate the stress distribution in the tile which is produced by ice formation. Furthermore, we will examine the influence of the other actual environmental conditions such as rain and solar radiation on the ice formation.

Acknowledgement

This study was supported by JSPS KAKENHI Grant Numbers 25870351 (Grant-in-Aid for Young Scientists (B)) and 56th Engineering Research Grants by Mizuho Foundation for the Promotion of Sciences.

References

- [1] C Iba, A Ueda, S Hokoi. Field Survey and Analysis on Frost Damage of Roof Tiles under Climatic Impact, International Symposium on Building Pathology; 2015;97-104.
- [2] Matsumoto M, Gao Y, Hokoi S. Simultaneous heat and moisture transfer during freezing-melting in building materials, CIB/W40 meeting, Budapest; 1993.
- [3] Iba C, Hokoi S. Frost Damage of Roof Tiles in Relatively Warm Areas in Japan: Influence of Surface Finish on Water Penetration, Proceedings of the Building Enclosure Science & Technology (BEST3); 2012